

CHAPTER ONE

INTRODUCTION

1.1 Background

Solar energy is radiant light and heat from the Sun that is harnessed using a range of ever-evolving technologies such as solar heating, photovoltaic, solar thermal energy, solar architecture, molten salt power plants, and artificial photosynthesis.

Solar energy is an important source of renewable energy and its technologies are broadly characterized as either passive solar or active solar depending on how they capture and distribute solar energy or convert it into solar power. Active solar techniques include the use of photovoltaic systems, concentrated solar power, and solar water heating to harness the energy. Passive solar techniques include orienting a building to the Sun, selecting materials with favorable thermal mass or light-dispersing properties, and designing spaces that naturally circulate air.

A solar cell, or photovoltaic cell, is an electrical device that converts the energy of light directly into electricity by the photovoltaic effect, which is a physical and chemical phenomenon. photoelectric cell is defined as a device whose electrical characteristics, such as current, voltage, or resistance, varying when exposed to light. Individual solar cell devices can be combined to form modules, otherwise known as solar panels. In basic terms, a single-junction silicon solar cell can produce a maximum open-circuit voltage of approximately 0.5 to 0.6 volts.

The spectral response of a solar cell is determined by illuminating the device with a series of monochromatic beams at different wavelengths and measuring the short-circuit current generated under each wavelength.

The responsivity of a solar cell is usually expressed in units of amperes per watt of incident radiant power. For a system that responds linearly to its input, there is a unique responsivity. For nonlinear systems, the responsivity is the local slope. Many common photodetectors respond linearly as a function of the incident power.

Responsivity of solar cell is a function of the wavelength of the incident radiation and of the sensory properties, such as the band-gap of the material of which the solar cell is made.

The term responsivity is also used to summarize the input-output relationship in non-electrical systems. For example, a neuroscientist may measure how neurons in the visual pathway respond to light. In this case, responsivity summarizes the change in the neural response per unit signal strength. The responsivity in these applications can have a variety of units. The signal strength typically is controlled by varying either intensity (intensity-response function) or contrast (contrast-response function). The neural response measure depends on the part of the nervous system under study. For example, at the level of the retinal cones, the response might be in photocurrent. In the central nervous system, the response is usually spiked per second. In functional neuroimaging, the response measure is usually a BOLD contrast. The responsivity units reflect the relevant stimulus and physiological units. When describing an amplifier, the more common term is gain. Deprecated synonym sensitivity. A system's sensitivity is the inverse of the stimulus level required to produce a threshold response, with the threshold typically chosen just above the noise level.

1.2 Research Problem

The sun emits energy in the form of electromagnetic waves. The wavelength of light have a significant influence on the performance of solar cell. Currently available solar cells respond well to some, but not all, wavelengths .Different solar cells are designed to operate efficiently at different wavelengths depending on the materials used to manufacture them. Research in the area of solar cells continues with an increasing interest to develop cells that will respond well at the widest range of wavelengths.

This work is focuses mainly on the spectrum response of silicon solar cell. and how to achieved the largest response or more wavelengths suitable for the solar cell to take advantage of the application of solar cell according to the result obtained by a solar cell was used to charge the phone battery and experiment with the appropriate tools.

1.3 Previous Studies

In 1979 HOVEL *et a*, used the fluorescent wavelength shifting to enhance the spectral response and AM0 conversion efficiency of several types of solar cells. Plastic fluorescent materials are useful for devices with a sharp cut-off in response, while ruby is suitable for devices with more gradual cut-offs. Efficiency improvements of 0.5 to 2 percentage points were measured on some cells, and greater improvements can be expected for optimized optical components. The optical efficiencies (light transmitted into the solar cell compared to light incident on the fluorescent sheet) exceeded 50% for the plastic sheets and 75% for ruby (HOVEL *et al*, 1979).

In 1998 Emery *et al*. discussed the various elemental random and nonrandom error sources in typical spectral responsivity measurement

systems. They focus specifically on the filter and grating monochromatic-based spectral responsivity measurement systems used by the Photovoltaic (PV) performance characterization team at NREL. A variety of subtle measurement errors can occur that arise from finite photo-current response time, the bandwidth of the monochromatic light, waveform of the monochromatic light, and spatial uniformity of the monochromatic and bias lights; the errors depend on the light source, PV technology, and measurement system. The quantum efficiency can be a function of the voltage bias, light bias level, and, for some structures, the spectral content of the bias light or location on the PV device. This paper compares the advantages and problems associated with semiconductor-detector-based calibrations and pyroelectric-detector-based calibrations. Different current-to-voltage conversion and ac photo-current detection strategies employed at NREL are compared and contrasted (Emery *et al*, 1998).

In 2007 Steven et al. measuring the absolute spectral irradiance responsivity of detectors have been compared between the calibration facilities at two national metrology institutes, the Helsinki University of Technology (TKK), Finland, and the National Institute of Standards and Technology (NIST). The emphasis is on the comparison of two different techniques for generating a uniform irradiance at a reference plane used wavelength-tunable lasers. At TKK's Laser Scanning Facility (LSF) the irradiance is generated by raster scanning a single collimated laser beam, while at the NIST facility for Spectral Irradiance and Radiance Responsivity Calibrations with Uniform Sources (CIRCUS), lasers are introduced into integrating spheres to generate a uniform irradiance at a reference plane. The laser-based irradiance responsivity results are compared to a traditional lamp-monochromatic-based irradiance responsivity calibration obtained at the NIST Spectral Comparator Facility (SCF). A narrowband

filter radiometer with a 24 nm bandwidth and an effective band-center wavelength of 801 nm was used as the artifact. The results of the comparison between the different facilities, reported for the first time in the near-infrared wavelength range, demonstrate agreement at the uncertainty level of less than 0.1%. This result has significant implications in radiation thermometry and in photometry as well as in radiometry. (Steven et al, 2007).

In 2009 Christian describes the measurement of the spectral response of digital cameras with a set of interference filters. The setup, processing of the data and the assessment of the measurement are discussed (Christian, 2009).

In 2010 Faisal et al. Studied effect of wavelength, the intensity of light and temperature factors on the output parameters of the silicon solar cell(short circuit current, open-circuit voltage, filling factor) they studied. The results indicate that the maximum practical value of efficiency by the effect of wavelength factor was equal (15.479%) at the wavelength (587nm) (yellow color) and light intensity(100W/m²) and temperature (296.5K). The maximum theoretical value of the efficiency was (79.533%) at the wavelength (452nm) (blue color) and light intensity (100W/m²) and temperature (296.5K) using a program in Visual –Basic language. The maximum practical value of efficiency by the effect of intensity factor was equal (22.214%) at the wavelength (509nm) (green color), and light intensity (600W/m²)and temperature (296.5K). The maximum theoretical value of the efficiency at the same conditions was equal (32.421%) by using the same program. Also, the results appeared that the maximum theoretical value of the efficiency at the same conditions was equal (24.618%) using the program characterization team at NREL. A variety of

subtle measurement errors can occur that arise from finite photo-current response time, the bandwidth of the monochromatic light, waveform of the efficiency at the same conditions was equal (32.421%) by used the same program. Also, the results appeared that the maximum theoretical value of the efficiency at the same conditions was equal (24.618%) used the program so the way is open to used some theoretical and practical factors to raise the efficiency of the solar cell (Feisal et al, 2010).

In 2012 Daisuke et al. used various methods of spectral responsivity measurements for dye-sensitized solar cells (DSCs) they investigated used two starkly different types of cells: one cell involving a 3-Methoxypropionitrile (MPN) as a solvent of an electrolyte and the other, an ionic liquid electrolyte. A linear relationship was observed between the short-circuit current and monochromatic light intensity in the range of 0.05 to 4.0 mW.cm⁻², not only for the MPN based cell but also for the ionic liquid-based cell, although the current response of the ionic liquid-based cell was slower probably due to the high electrolyte viscosity. It was found that correct spectral responsivity measurements could be performed by a conventional AC method in which the chopping frequency was adjusted low enough to obtain a steady-state current under illumination conditions similar to practical applications. While the spectral responsivity determined by the DC method was higher than that by the AC method under white bias irradiation. The DC method considered useful to compare the spectral responsivity of DSCs prepared by different manufacturers since errors caused by the use of a different bias light source by individual manufacturers would be eliminated (Daisuke et al, 2012)

In 2014 Marouf *et al*, utilized fast laser texturing technique to produce micro/nano surface textures in Silicon photovoltaic cell by means of UV

femtosecond laser pulses, in order to match the modern technological components to the scale, proportion, material, color scheme and balance of buildings. The experimental evidence of the effect of femtosecond laser pulses on the spectral response of Silicon photovoltaic cells are demonstrated and investigated. The response of that device is covering the visible to near-infrared spectral region. The responsivity of the photovoltaic cell is up to 0.25 A/W (Marouf, 2014).

In 2018 Joseph et al, Improved spectral modification for applications in tow solar cells, the spectral mismatch between solar cells and incident radiation is a fundamental factor limiting their efficiencies. There exist materials and luminescent processes, which can modify the incident sunlight's properties to better suit the cell's optimal absorption regions. This makes for an interesting area of research and promising technique for enhancing the efficiency of solar cells, which is important for environmental reasons. It is intended for this review to provide the reader with historical and up-to-date developments of the application of spectral modification to solar cells and contribute to growing its impact on real-world PV devices. They concisely outline the underlying principles of three spectral modification processes: up-conversion, down-conversion and luminescent down-shifting (LDS). For each section, they present up to date experimental results for applications to a range of solar PV technologies and discuss their drawbacks. With a particular focus on up-conversion, they then review how nanostructures or integrated optics might overcome these problems. Finally, they discuss practical challenges associated with advancing this approach for commercialization and opportunities spectral modification presents; namely, where future research should focus and via a cost analysis with a simple form (Joseph et al, 2018).

In 2018 Liaet et al, Achieved full spectral response by utilizing the near-infrared (NIR) and ultraviolet (UV) parts of sunlight have undoubtedly become an important focus on increasing the power conversion efficiency (PCE) of perovskite solar cells (PSCs). Introducing a photoluminescent conversion layer by converting NIR or UV light into visible which can be effectively utilized by perovskite photoactive layer has been considered as a very promising route. In this work, on the basis of a novel NiO/Ag/NiO transparent electrode, the NaYF₄: Yb₃⁺, Er₃⁺/NaYF₄: Yb₃⁺, Tm₃⁺/ Ag composite layers were introduced on the backlight side of the PSCs device by the pulsed laser deposition (PLD). This design enables multi-functional effects, harvesting NIR light and converting to visible, plasmonic scattered, reflection and luminescent enhancement. In this device, they observed a considerable enhancement of PCE depending strongly on the power density of sunlight. Simultaneously, acting as an efficient encapsulation layer, the device also greatly boosted the long-term stability of PSCs in ambient conditions. Furthermore, a typical UV to visible Eu(TTA)₂(Phen)MAA down-conversion (DC) layer was introduced on the incident light side of PSCs, leading to improvement of PCE and light stability of PSCs. Overall, the upconversion (UC) and DC effects give rise to the highest PCE performance of 19.5% and noticeable current density (J_{sc}) value of 27.1mA.cm⁻² among the reported transparent PSCs, suggesting the great potential for application in spectral broadening and stability enhancement of PSCs.upconversion (UC) and DC effects give rise to the highest PCE performance of 19.5% and noticeable current density (J_{sc}) value of 27.1mAcm⁻² among the reported transparent PSCs, suggesting the great potential for application in spectral broadening and stability enhancement of PSCs.that can be used to determine financial viability for the deployment of this technology (Liaet et al,2018)

In 2018 Fengyou et al, Boosted spectral response of multi-crystalline Si solar cells with Mn_2^+ doped CsPbCl_3 quantum dots down converter

Conventional multi-crystalline Si solar cells present limited spectral response in the near-ultraviolet region due to the parasitic absorption caused by passivation layer and heavily doped emitter player. Converting ultraviolet light into visible light is a promising way to improve the performance of the devices. Herein, $\text{CsPbCl}_3: \text{Mn}_2^+$ quantum dots are applied on to the front of the multi-crystalline Si solar cells as the luminescent down converter to improve light harvesting in the short wavelength region. $\text{CsPbCl}_3: \text{Mn}_2^+$ quantum dots with large Stokes shift ($>1000\text{meV}$) and high quantum yield (62%) effectively convert the normally low responding spectral in the ultraviolet region into usable visible light at $\sim 600\text{nm}$ for improving photoelectric conversion efficiency of the devices. Combining with the unique light-trapping architecture of multi-crystalline Si solar cells, external quantum efficiency in the ultraviolet region is evidently improved, leading to an increased conversion efficiency of 6.2%. Meanwhile, solar cells coated with $\text{CsPbCl}_3: \text{Mn}_2^+$ quantum dots luminescent down converter layer also exhibit favorable photostability under AM 1.5G illumination and reproducibility. Based on these characteristics, they deem this light-management strategy could be applied on mass product multi-crystalline Si solar cells, and easily extended to enhance the performance of other solar cells (Fengyou et al, 2018).

1.4 Objectives of this Dissertation

This work aims to Measure of the Spectral Response of Silicon Solar Cell with a Set of Filters , with additional objective of improve efficiency of Silicon Solar Cell. The main objectives of this research are to:

1. Carried out the I/V characteristics experiment of silicon solar cell.

2. Measure the spectral responsivity of silicon solar cell for some visible spectra.
3. Plot the wavelength current relation of the silicon solar cell.
4. Calculate the power and efficiency of the silicon solar cell.
5. Identify the higher spectral range responsivity of the silicon solar cell.

1.5 Research Methodology

To achieve the objectives of this dissertation, a silicon solar cell will be connected in I/V characteristic circuit, and Rheostat, Filters, The solar cell will be connected in series with the current and the voltage parallel. The filters will subject to each filter separately and the spectral range will take and the results will be recorded in a table. The graph will draw to determine the best spectral response.

1.6 Dissertation Layout

This dissertation is is organized into four chapters, chapter one presents background theory and a literature review of the Spectral Response of Silicon Solar Cell, and chapter two consist Basic Concepts of cell and responsivity spectrum, chapter three describes the basic equipments described in detail and experimental setup implementation. In order to verify measurement of Spectral Response of Silicon Solar experimentally the equipments and setup are implemented on a practical test rig. chapter four presents the experimental results of measurement of Spectral Response test, Discussion, and draws general conclusions and provides suggestions for further research work in this area.

CHAPTER TWO

BAISC CONCEPTS

2.1 Solar Energy

Solar radiation is a renewable energy resource that has been used by humanity in all ages. Passive solar technologies were already used by ancient civilizations for warming and/or cooling habitations and for water heating; in the Renaissance, concentration of solar radiation was extensively studied and in the 19th century solar-based mechanical engines were built and photovoltaic effect.

2.1.1 Introduction

In the time when the world is debating on climate change issues which is basically due to the use of fossil fuel, the use of solar energy in various form is relevant. The existing buildings are responsible to the use of a large amount of energy for lighting, heating, cooling, and use of various energy run equipment mostly powered by fossil energy. recent intention should be to replace the fossil fuel by solar energy which is free and available in abundance. Now, solar technologies in the form of photovoltaic's and thermal collectors are available in competitive prices. However, their use has not been to the expectation especially in the building sector to replace the use of fossil fuels. The main reason for these technologies not being popular in building integration is the lack of good architectural quality rendered not meeting desired design considerations. Innovative approaches have to be explored in terms of design and implementation in order to match the modern technological components to the scale, proportion, material, color scheme, and balance of buildings. Therefore, the objective of this thesis is to pave possible ways of

integrating these technologies into buildings, both on existing and new constructions to add emphasis to the overall architectural expression in addition to producing energy. The intention here is to highlight design possibilities regarding the use of solar technologies into buildings with innovative approaches. The basic focus is on the appearance or aesthetics part of integration as this makes the major impact on the people. PVs and thermal collectors can deliberately be used as architectural design elements in a distinctive way. The development towards the passive house, zero energy, and zero-emission buildings will cause a more frequent use of building-integrated solar energy systems as a source of renewable energy. Due to the limitations in the integrability of such systems in relation to the design, color, and scale of the building envelope, their integration may ruin the final architectural quality of the building. Many solar systems do exist on the market, and with better and better energy performance. Nevertheless, if they are not designed to be integrated into buildings to enhance the quality of architecture, probably no one will opt using. These systems as a source of renewable energy generators. In this case, even though there will be more and more efficient PV or stander test condition (STC) systems in the market, they will not have used if aesthetic ways of integrating them are not sought. It looks like PV integration has brought about some improvements in the architectural quality of building integration, but the solar thermal collectors lack on this part to some extent. While the technical development and energy performance improvements are always in progress, the actual use of these systems in buildings is not increasing as it could and should do. Existing buildings account for over 40% of the world's total primary energy use and 24% of greenhouse gas emissions. A combination of making buildings more energy-efficient and using a larger fraction of renewable energy is, therefore, a key issue to

reduce non-renewable energy use and greenhouse gas emissions. With this aim, the integration of PV and solar thermal collector systems into buildings becomes very important. Integrating these PV and solar thermal collectors systems into buildings is not only for clean energy but also to use them as multifunctional elements where they replace the conventional building elements. With this, the economic viability of integration is met and most importantly, they become architectural components. Therefore, the possible ways of architectural integration of PV and solar thermal collector systems have been explored and analyzed. A special focus made on the aesthetic part of the integration. 'Integrability' of both the systems in terms of different integration requirements has been compared. In doing so, the integration advantages of both systems have been explored. Solar energy is created by light and heat which is emitted by the sun, in the form of electromagnetic radiation. With today's technology, we are able to capture this radiation and turn it into usable forms of solar energy - such as heating or electricity. Solar energy is the sun's nuclear fusion reactions within the continuous energy generated. Earth's orbit, the average solar radiation intensity is $1367\text{kw}/\text{m}^2$. Circumference of the Earth's equator is 40000km , thus we can calculate the energy the earth gets is up to $173,000\text{ TW}$. At sea level on the standard peak intensity is $1\text{kw}/\text{m}^2$, a point on the earth's surface 24h of the annual average radiation intensity is $0.20\text{kw}/\text{m}^2$, or roughly $102,000\text{ TW}$ of energy. Humans rely on solar energy to survive, including all other forms of renewable energy (except for geothermal resources) Although the total amount of solar energy resources is ten thousand times of the energy used by humans, but the solar energy density is low, and it is influenced by location, season, which is a major problem of development and utilization of solar energy (Wall, 2009).

2.1.2 Available Solar Resource

The technical feasibility and economic viability of using solar energy depend on the amount of available sunlight (solar radiation) in the area where you intend to place solar heaters or solar panels. This is sometimes referred to as the available solar resource. Every part of Earth is provided with sunlight during at least one part of the year. "Part of the year" refers to the fact that the north and south polar caps are each in total darkness for a few months of the year. The amount of sunlight available is one factor to take into account when considering using solar energy. There are a few other factors, however, which need to be looked at when determining the viability of solar energy in any given location. These are as follows:

- Geographic location
- Time of day
- Season
- Local landscape
- Local weather

Day and night are due to the Earth's rotation, but the season is due to the Earth's rotation axis and the Earth's orbit around the sun's axis at a 23°27' angle and generated. The Earth rotates around the "axis" which through its own north and south poles a circuit from west to east every day. Per revolution of the earth cause day and night, so the Earth's rotation per hour is 15°. In addition, the Earth goes through a small eccentricity elliptical orbit around the sun per circuit per year. The Earth's axis of rotation and revolution has always been 23.5° with the earth orbit. The Earth's revolutions remain unchanged when the direction of the spin axis always points to the Earth's the North Pole. Therefore, the Earth's orbit at a different location when the sunlight is projected onto the direction

of the earth is different, so it causes the formation of the Earth's seasons changes. Noon of each day, the sun's height is always the highest. In the tropical low-latitude regions (in the equatorial north and south latitude 23° ~ 27° between the regions), the sunlight of each year, there are two vertical incidences at higher latitudes; the sun is always close to the equator direction. In the Arctic and Antarctic regions (in the northern and southern hemispheres are greater than 90° ~ 23° ~ 27°), in winter the sun below the horizon for a long time (bachelor,2010).

2.2 Solar Cell

A solar cell (photovoltaic cell) is a solid-state electronic device that takes in light energy and converts it directly into electrical energy. This is sort of like a light bulb that is acting in reverse.

The typical blue/silver solar cell has a base of the element silicon. The silicon is doctored so that some loosely held electrons in the silicon could be bounced into the electrical circuit. These moving electrons, also known as electrical current, can power electronic devices, especially devices that have low power requirements. Low power devices would be things like calculators, radios, LED lights, electronic switches, monitoring equipment, rechargers for batteries, and such. Solar cells have made space habitation and space research possible. The International Space Station gets its electrical power from massive arrays of solar cells. Similarly, the earlier Space Lab and Mir Space Stations also used solar power. The Space Shuttle does not use solar cells but uses fuel cells, which produces drinking water as a by-product. Most satellites orbiting the earth use solar cells for power. Planetary probes go away from the earth and sun and the light intensity diminishes, so they do not rely on solar power but use other power sources (Trondheim, 2012).

2.2.1 Principle of solar cell

The basic element of solar panels is pure silicon. When stripped of impurities, silicon makes an ideal neutral platform for transmission of electrons. In silicon's natural state, it carries four-electron but has room for eight. Therefore, silicon has room for four more electrons. If a silicon atom comes in contact with another silicon atom, each receives the other atom's four electrons. Eight electrons satisfy the atoms' needs, this creates a strong bond, but there is no positive or negative charge. This material is used on the plates of solar panels. Combining silicon with other elements that have a positive or negative charge can also create solar panels. For example, phosphorus has five electrons to offer to other atoms. If silicon and phosphorus are combined chemically, the results are a stable eight electrons with an additional free electron. The silicon does not need the free electron, but it cannot leave because it is bonded to the other phosphorous atom. Therefore, this silicon and phosphorus plate is considered to be negatively charged.

A positive charge must also be created in order for electricity to flow. Combining silicon with an element such as boron, which only has three electrons to offer, creates a positive charge. A silicon and boron plate still has one spot available for another electron. Therefore, the plate has a positive charge. The two plates are sandwiched together to make solar panels, with conductive wires running between them.

Photons bombard the silicon/phosphorus atoms when the negative plates of solar cells are pointed at the sun. Eventually, the 9th electron is knocked off the outer ring. Since the positive silicon/boron plate draws it into the open spot on its own outer band, this electron does not remain free for long. As the sun's photons break off more electrons, electricity is then

generated. When all of the conductive wires draw the free electrons away from the plates, there is enough electricity to power low amperage motors or other electronics, although the electricity generated by one solar cell is not very impressive by itself. When electrons are not used or lost to the air they are returned to the negative plate and the entire process begins again (Bachelor's, 2010)

2.2.2 Applications of solar cell

2.2.2.1 Utility Interactive Applications

In utility interactive (or grid-connected) PV systems have become increasingly popular for building integrated applications. As illustrated in Figure 2.1, they are connected to the grid via inverters, which convert the DC power into AC electricity. This electricity can then power household appliances or can be sold directly to the grid. As a building receives this energy, it is distributed to appliances and lighting, or other devices where needed. Since PV systems are restricted to function only exposed to the sun, a backup system is frequently required to ensure a continuous supply of electricity irrespective of the weather conditions. These systems are most commonly used in houses or commercial buildings to offset electricity cost. A well-designed PV system with a proper storage facility can be an attractive prospect for displacing power during peak hours.

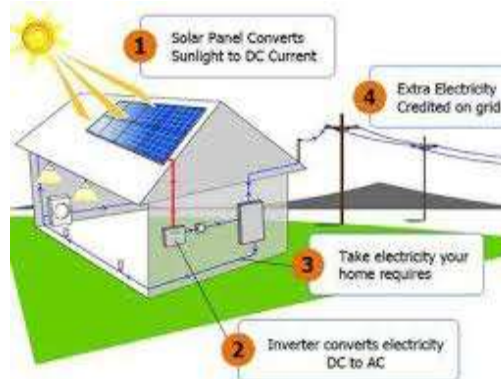


Figure: 2.1 Schematics of utility-interactive applications

2.2.2.2 Stand-Alone Systems

Stand-alone systems directly use the generated produced electricity. These systems can consist of the PV modules and a load only or they can include batteries for energy storage Stand-alone systems do not rely on utility/grid connections. When the requirement arises during the nighttime or poor sunlight, a battery storage system is used. In some situations, stand-alone systems use conventional generators as backup systems.

2.2.2.3 Lighting

With the invention of LED (light-emitting diode) technology as low power lighting sources, PV systems find an ideal application in remote or mobile lighting systems. PV systems combined with battery storage facilities are mostly used to provide lighting for billboards, highway information signs, public-use facilities, parking lots, vacation cabins, lighting for trains. Figure 2.2 shows schematically example of application of streetlight powered by PV system and Figure 2.3 shows Portable lighting system along with mobile charging facility.



Figure:2.2 A street light powered by PV



Figure:2.3 Portable lighting system along with mobile charging facility

2.2.2.4 Communication

In the current modern era, artificial satellites are considered as one of the greatest mankind creations. Satellites are used for several services and applications like broadcasting satellite services (BSS), fixed satellite services (FSS), remote sensing and earth observation services, meteorological and navigation services, search and rescue operations in addition to the space telescopes and the military purposes. The Solar Power Satellite energy system is to place giant satellites, covered with vast arrays of solar cells. Photovoltaic solar arrays are the prime way of converting the solar energy to an efficiently electrical energy for satellites. Array configurations depend on the spacecraft stabilization concept, the orbit type, and the power requirements. Figure 2.4 illustrates Satellites used for communication are powered by PV.

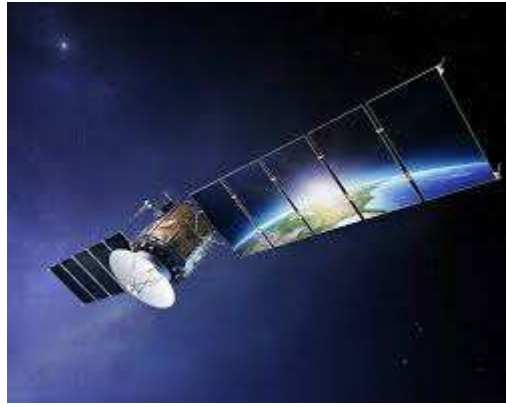


Figure:2.4 Satellites used for communication are powered by PV

2.2.2.5 Electricity for remote areas

Some areas are quite far from the distribution network to establish a connection with the grid. Areas under construction also need power supply before they are connected. Figure 2.5 rural area is powered by PV system. PV systems are an attractive option for rural area. Furthermore, PV systems can provide a back up for conventional generators.



Figure:2.5 Remote area in Africa powered by PV

2.2.2.6 Disaster Relief

Natural calamities often bring about an electricity crisis. Disasters such as hurricanes, floods, tornadoes, and earthquakes destroy electricity

generation and distribution systems. In situations like these, where power will be out for an extended period, portable PV systems which are illustrated in Figure 2.6 can provide temporary solutions for light, communication, food and water systems. Emergency health clinics opt for PV based electricity over conventional systems in lieu of problems of fuel transport and pollution.



Figure:2.6 Portable PV systems powering area struck by a natural disaster

2.2.2.7 Scientific experiments

In various cases, scientific experiments are set up in areas far from the power supply. PV systems can be effectively used to carry out scientific activities in remote areas. Systems monitoring seismic activities, highway conditions, meteorological information, and other research activities can be powered by PV systems.

2.2.2.8 Signal Systems

Navigational systems, such as lighthouses, highway and aircraft warning signals can be far from the electric grid. PV systems can be a reliable power source for these important applications. Even portable traffic lights can be powered by PV systems.

2.2.2.9 Water Pumping

Photovoltaic (PV) panels are often used for agricultural operations, especially in remote areas or where the use of an alternative energy source is desired. In particular, they have been demonstrated time and time again to reliably produce sufficient electricity directly from solar radiation (sunlight) to power livestock and irrigation watering systems. A benefit of using solar energy to power agricultural water pump systems is that increased water requirements for livestock and irrigation tend to coincide with the seasonal increase of incoming solar energy. When properly designed, these PV systems can also result in significant long-term cost savings and a smaller environmental footprint compared to conventional power systems. Figure: 2.7 illustrated a typical solar-powered water pump system, which includes a solar array, controller, pump, and storage tank. Solar water pumps can be very cost-effective for remote agricultural activities.

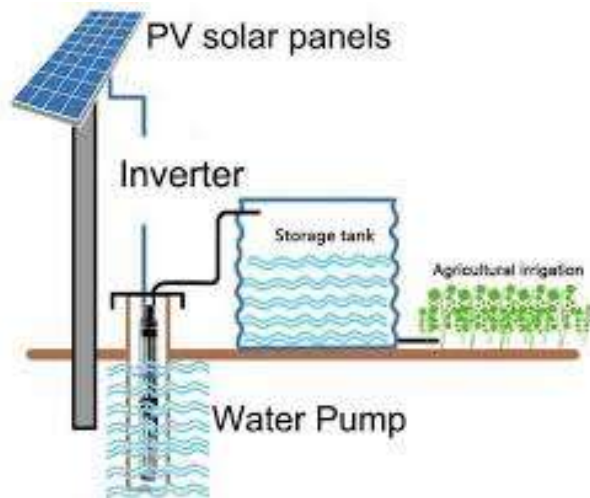


Figure: 2.7 a typical solar-powered water pump system

2.2.2.10 Charging Vehicle Batteries

Vehicles running on electric power can be charged at PV powered stations. Such vehicles can also maintain their critical battery states using

PV powered sources. Boats and other leisure vehicles can be charged directly using PV systems

2.2.2.11 Solar Power Cathodic Protection

The principle of cathodic protection is based on the idea to reverse the electrochemical role of the structure to be protected by supporting a cathodic reduction on its level, and by deferring the reaction of oxidation on another structure which we accepts the degradation. Pipelines, wellheads and other metallic structures are prone to corrosion due to exposure to water. Corrosion occurs due to the electrolytic activity of metals as they lose ions in contact with water. This electrolytic process leading to corrosion can be reduced by applying an external voltage. This external voltage will prevent the ion loss from the metal. To that end, only a small DC voltage will be enough. PV is a suitable candidate for this purpose as they produce low voltage DC power that can be used directly. Cathodic protection using PV is illustrated in Figure 2.8.



Figure:2.8 Cathodic protection using PV

2.2.2.12 Refrigeration

A rational use of energy brings both economic and environmental benefits, by reducing consumption of fossil fuels, electricity and pollutant emissions. PV-powered refrigeration system that eliminates reliance on an

electric grid, requires no batteries, and stores thermal energy for efficient use when sunlight is absent. The PV-powered refrigeration system, which is illustrated in Figure 2.9, uses a variable speed, direct current (DC) vapor compression cooling system, connected to a solar photovoltaic (PV) panel via novel electronic controls. This environmentally friendly system is ideal for use in commercial or household refrigerators, freezers, vaccine coolers, or solar ice-makers. PV system can be exceptionally suitable for storage and transport of medicines and vaccines that require refrigeration.



Figure:2.9 Solar powered refrigerator

2.2.2.13 Consumer Products

PV technology is being used for a variety of commercially available consumer-based products. Small DC appliances such as toys, watches, calculators, radios, televisions, flashlights, fans, etc. can operate with PV based energy systems, which are illustrated in Figure 2.9



Figure:2.10 Solar powered calculator and radio

2.2.2.14 Public utilities

Various public utility systems such as teller machines and telephone booths can also be powered by PV systems. A typical Automatic Teller Machine (ATM) and telephone systems booth powered by PV are represented in Figure 2.11.



Figure:2.11 ATM and telephone booth powered by PV

2.2.3 Types of solar cell

Solar cells are typically named after the semiconducting material they are made of. These materials must have certain characteristics in order to absorb sunlight. Some cells are designed to handle sunlight that reaches the Earth's surface, while others are optimized for use in space. Solar cells can be made of only one single layer of light-absorbing material (single-junction) or use multiple physical configurations (multi-junctions) to take advantage of various absorption and charge separation mechanisms. Solar cells can be classified into first, second and third generation cells. The first generation or wafer-based cells are made of crystalline silicon, the commercially predominant PV technology, that includes materials such as polysilicon and monocrystalline silicon. Second generation cells are thin film solar cells, that include amorphous silicon, CdTe and CIGS cells and

are commercially significant in utility-scale photovoltaic power stations, building integrated photovoltaics or in small standalone power system. The third generation of solar cells includes a number of thin-film technologies often described as emerging photovoltaics most of them have not yet been commercially applied and are still in the research or development phase. Many use organic materials, often organometallic compounds as well as inorganic substances.

2.2.3.1 Photovoltaic Cells

Photovoltaic systems are sustainable, environmentally friendly, quiet, and light and require minimal maintenance, as they have no moving parts. In a PV system, cells combine to form modules, which give the system the flexibility to be expanded or reduced to suit any given application. The versatility of PV panels gives numerous possibilities for their integration into new and existing structures. Although the most commonly used cell types come from the same base material silicon, different technologies offer cells with different technical and aesthetic characteristics.

2.2.3.2 Mono-crystalline cells

The mono-crystalline silicon solar cell is made of a large single crystal of pure silicon. This single crystal is mostly fabricated into thin wafers from a singular continuous crystal. To minimize waste, the cells may be fully round or they may be trimmed into other shapes, retaining more or less of the original circle. A single crystal has a uniform color (Solar, 2011). Mono-crystalline silicon modules normally appear as a solid color, ranging from blue to black. A wide variety of colors is available but these are of lower efficiency. Magenta or gold results in a loss of 20% efficiency. These cells are around 10 x 10 cm² and 350 microns in thickness with an efficiency of

up to 14-17%. They produce, on average in European weather, 900-1000 kWh per each kW installed.

2.2.3.3 Poly-crystalline cells

Polycrystalline cells are made from similar silicon material to that of the mono-crystalline except that instead of being grown into a single crystal, they are melted and poured into a mold. This forms a square block that can be cut into square wafers with less waste of space or material than round single-crystal wafers. As the material cools, it crystallizes in an imperfect manner, forming random crystal boundaries (Solar, 2011).

2.2.3.4 Thin-film cells

This latest technology of thin film either is from silicon or produced from new base materials, such as Gallium- Arsenide (GaAs), Cadmium-Telluride (CdTe) or Copper-Indium-Diselenide (CIS). These cells also called amorphous (Solar, 2011) protected by means of encapsulation with front glass and back protection, resulting in PV modules. Thin-film cells have efficiencies up to 5-8% and produce an average 600-800 kWh per each kW installed and are available in a range of colors.

2.2.3.5 PV modules

PV cells are arranged together to form modules as shown in Figure 2.12. The modules are designed for outdoor conditions, so they are able to be part of the building skin. However, different encapsulation technologies result in a range of PV panels having different performances as a constructive element like glass-plastic or glass-glass back sheet. Standard modules have an aluminum frame. Modules without a frame also called "laminates", are more commonly used for building integration. The production of solar panels technologies are illustrated in Figure 2.13,

which is distinguish mainstream technologies: Solid crystallized materials
Amorphous and thin film materials.



Figure:2.12 PV modules

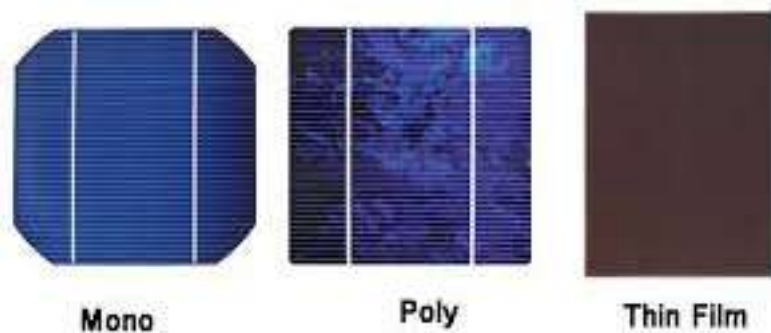


Figure: 2.13 technologies of solar cell

2.3 Responsivity

A response spectrum is a plot of the peak or steady-state response (displacement, velocity or acceleration) of a series of oscillators of varying natural frequency, that are forced into motion by the same base vibration or shock. The resulting plot can then be used to pick off the response of any linear system, given its natural frequency of oscillation. One such use is in assessing the peak response of buildings to earthquakes. The science of strong ground motion may use some values from the ground response spectrum (calculated from recordings of

surface ground motion from seismographs) for correlation with seismic damage.

If the input used in calculating a response spectrum is steady-state periodic, then the steady-state result is recorded. Damping must be present, or else the response will be infinite. For transient input (such as seismic ground motion), the peak response is reported. Some level of damping is generally assumed, but the value will be obtained even with no damping.

Response spectra can also be used in assessing the response of linear systems with multiple modes of oscillation (multi-degree of freedom systems), although they are only accurate for low levels of damping. Modal analysis is performed to identify the modes, and the response in that mode can be picked from the response spectrum. These peak responses are then combined to estimate a total response. A typical combination method is the square root of the sum of the squares (SRSS) if the modal frequencies are not close. The result is typically different from that which would be calculated directly from an input since phase information is lost in the process of generating the response spectrum.

The main limitation of response spectra is that they are only universally applicable for linear systems. Response spectra can be generated for non-linear systems, but are only applicable to systems with the same non-linearity, although attempts have been made to develop non-linear seismic design spectra with the wider structural application. The results of this cannot be directly combined for a multi-mode response.

Response spectra are very useful tools of earthquake engineering for analyzing the performance of structures and equipment in earthquakes since many behave principally as simple oscillators (also known as a single degree of freedom systems). Thus, if you can find out the natural

frequency of the structure, then the peak response of the building can be estimated by reading the value from the ground response spectrum for the appropriate frequency. In most building codes in seismic regions, this value forms the basis for calculating the forces that a structure must be designed to resist (seismic analysis).

As mentioned earlier, the ground response spectrum is the response plot done at the free surface of the earth. Significant seismic damage may occur if the building response is 'in tune' with components of the ground motion (resonance), which may be identified from the response spectrum. This was observed in the 1985 Mexico City Earthquake where the oscillation of the deep-soil lake bed was similar to the natural frequency of mid-rise concrete buildings, causing significant damage. Shorter (stiffer) and taller (more flexible) buildings suffered less damage.

In 1941 at Caltech, George W. Housner began to publish calculations of response spectra from accelerographs. In the 1982 EERI Monograph on "Earthquake Design and Spectra". Newmark and Hall describe how they developed an "idealized" seismic response spectrum based on a range of response spectra generated for available earthquake records. This was then further developed into a design response spectrum for use in structural design, and this basic form (with some modifications) is now the basis for structural design in seismic regions throughout the world (typically plotted against structural "period", the inverse of frequency). A nominal level of damping is assumed (5% of critical damping). For "regular" low-rise buildings, the structural response to earthquakes is characterized by the fundamental mode (a "waving" back-and-forth), and most building codes permit design forces to be calculated from the design spectrum on the basis of that frequency, but for more complex structures, combination of the results for many modes (calculated

through modal analysis) is often required. In extreme cases, where structures are either too irregular, too tall or of significance to a community in disaster response, the response spectrum approach is no longer appropriate, and more complex analysis is required, such as non-linear static or dynamic analysis like in seismic performance analysis technique.

The typical earthquake ground motion response spectrum represents an envelope of the peak responses of many single-degree-of-freedom (SDOF) systems with different periods. The acceleration response spectrum of ground motion is a relationship between the natural period of vibration of an of the system and the maximum absolute acceleration that it experiences under the ground motion. Similarly, a displacement response spectrum typically represents the peak displacement, relative to the ground, of many systems with different periods. Hence, the construction of a response spectrum involves the analysis of many different of systems. The value of each point on the spectrum is the peak response of a single degree of freedom system of a given period. Ts is illustrated in figure 2.14, where the displacement spectrum of a record from the Palm Springs Earthquake is shown, along with the time history response at several periods. The relationship between the peak response at the different periods and the spectrum is graphically illustrated.

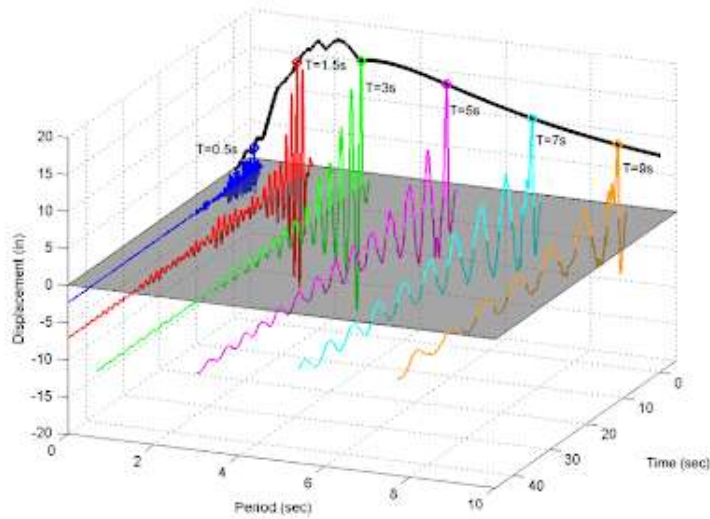


Figure 2.14: Construction of linear displacement spectra for a record from the 1986 North Palm Springs earthquake. The displacement histories are shifted to make the peak displacements coincide with the time origin (Caltech et al,1941).

The most commonly used forms of linear spectra are:

Acceleration spectra “Sa” (Sa vs. T),

Displacement spectra “Sd” (Sd vs. T),

Velocity spectra “Sv” (Sv vs. T).

Other commonly used spectra are pseudo-acceleration spectra “PSA” and pseudo-velocity spectra “PSv”, which are easily derived from the displacement spectra using the following equations:

$$PSv = \omega * Sd \quad (2.1)$$

$$PSA = \omega * PSv = \omega^2 * Sd \quad (2.2)$$

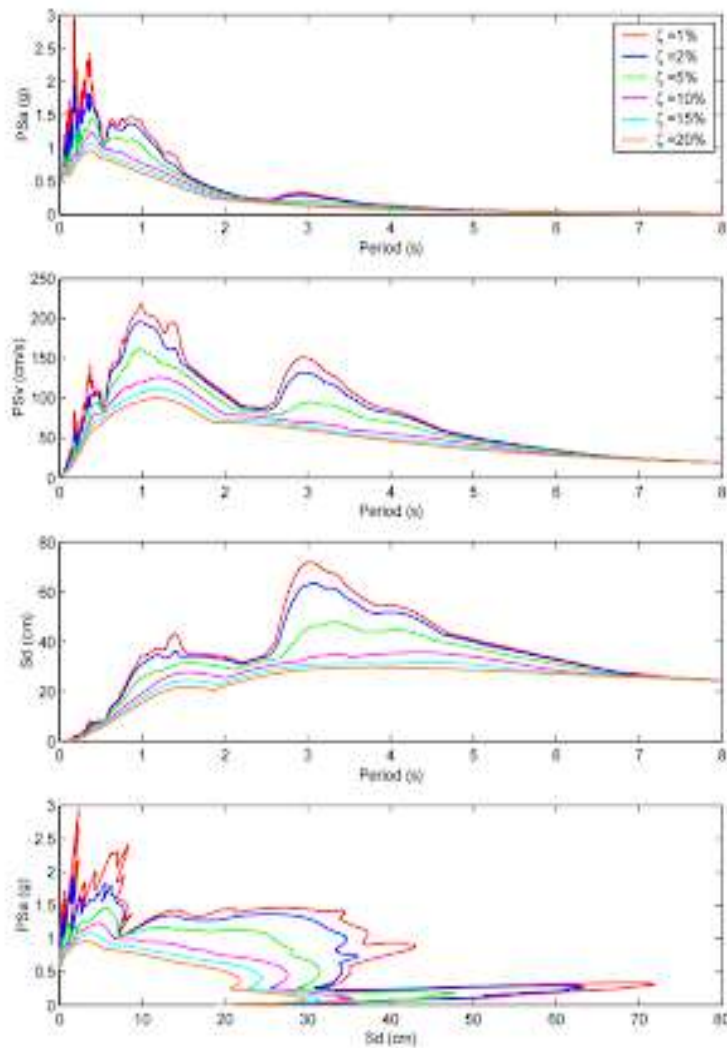


Figure: 2.15 PSA, PSv, Sd and ADRS spectra for the 1994 Northridge Rinaldi record, for multiple damping values.

The spectral responsivity or quantum efficiency (QE) is essential for understanding the current generation, recombination, and diffusion mechanisms in photovoltaic devices. PV cell and module calibrations often require a spectral correction factor that uses the QE. The quantum efficiency in units of electron-hole pairs collected per incident photon is computed from the measured spectral responsivity in units of amps per

watt as a function of wavelength. Typically, the spectral response is measured at short-circuit current. The measured photo-current is often in the μA to mA range with a broadband DC bias light near the devices intended operating point e.g. 1-sun. PV devices normally operate near their maximum power point; this is not normally a problem except in the case of amorphous silicon where the QE is voltage-dependent. (CUREE, 1997).

Spectral responsivity (SR) can be calculated as in (2.3)

$$S(R) = I_m/P_m(\lambda) \quad (2.3)$$

Where $S(R)$ is responsivity spectra, I_m is short circuit current, and P_m is incident light power.

In addition, the relationship between quantum Efficiency and responsivity spectra for solar cell V is find as in (2.4).

$$QE(\lambda) = N_{sig}(\lambda) / [N_{ph}(\lambda)] \quad (2.4)$$

Where N_{sig} is the generation of charge for any point area per unit, N_{ph} is Number of the incident photon.

$$N_{sig} = I_p \cdot A_{pix} \cdot t_{int} / e \quad (2.5)$$

$$N_{ph} = P \cdot A_{pix} \cdot t_{int} / hu \quad (2.6)$$

Where, P_{in} is generation current(A/cm^2), A_{pix} : solar cell area(cm^2),

P is the incident power(W/cm^2), t_{int} :stream integration and e is electron charge

From this we can definition the reponsivity spectra it is ratio between generation and the incident power in (2.6)

$$SR(\lambda) = I_{ph}[A/\text{cm}^2]/p[w/\text{cm}^2] = qN_{sig}/(h\nu N_{ph}) = QE. e\lambda/hc \quad (2.6)$$

CHAPTER THREE

EXPERIMENTAL PART

3.1 Introduction

In order to verify the Measurement of the Spectral Response of Silicon Solar Cell with a Set of Filters experimentally a setup is implemented in the laboratory. This chapter details the experimental setup. In this chapter the experimental equipments are used to perform the standard Responsivity test and the equipments are described.

3.2 Equipments

The experimental setup of the spectral response measurement constructed for the aim of this work contains of: silicon solar cell, Rheostat, Filters, and Light source.

3.2.1 Solar cell

The solar cell that used in this work was silicon solar cell with dimensions of 9.6x6.6cm, Model: cis-YT005 120000, capacity: 3.7v / 37wh, Input: DC 5V=1A (MAX) Solar: 25W, Output1: DC5V:1.0A (MAX) Output2: DC5V: 2.1A (MAX) Made in China as shown in figure 3.1.



Figure3.1: the silicone solar cell charge battery.

3.2.2 Rheostat

Figure 3.2 shows the rheostat (potentiometer) used to have variables values of voltage, it's maximum resistant is 11 OHM and current 3.3A.



Figure:3.2 Rheostat 6 OHM, 4A.

3.2.3 Filters

Five filters used in this experiment are illustrated in figure 3.3, they were as follow red 620 nanometers, orange 585 nanometers, yellow 570 nanometers, green 490 nanometers, blue 440 nanometers, Violet 400 nanometer.



Figure:3.3 Filter.

3.2.4 Light source

The light source was a tungsten 100/W lamp.

3.3 Experimental Setup

In this experiment, the solar cell is connected directly to the short circuit current and in parallel with the open-circuit voltage. The short circuit voltage is connected with the variable resistance (rheostat) and then a light source was placed on 50cm from the solar cell and 27cm from the filter. The short circuit current and the open-circuit voltage were recorded with changing of resistance each time and the reading was recorded in a table. These steps were repeated six times using the six filters (red (620), orange (585), yellow (570 nm), green (490 nm), blue (440 nm) and violet (400 nm)), they were exposed to the same light intensity. The experimental set-up is as shown in Figure 3.1.



Figure: 3.4 The experimental set-up

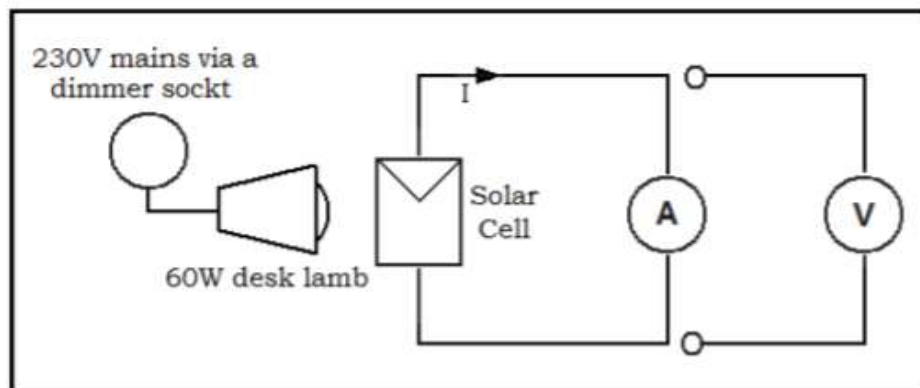


Figure :3.5 Circuit for measuring the current-voltage characteristic.

3.4 Characteristic Curves of Solar Cell

Usually, there are four a variable used for studying out of the solar cell, these variables are:

3.4.1 Short Circuit Current

Is the current through the solar cell when the voltage across the solar cell is zero (when the solar cell is short-circuited). It is due to the generation and collection of light-generation carriers. For an ideal solar cell most moderate resistive loss mechanisms, the short-circuit and the light-generation current are identical. The short circuit current is the largest current, which may be drawn from the solar cell. The current is generated by the solar cell is given as in 3.1.

$$I_{SC} = I_o \left(e^{qV_{oc}/KT} - 1 \right) \quad (3.1)$$

Where I_o is dark saturation current, q is an electronic charge, V has applied a voltage across the terminals of the diode, k is Boltzmann's constant, T is temperature I_L is light-generated current.

3.4.2 open-circuit voltage

This is the voltage corresponds to the open circuit condition when the impedance is high and is calculated when the current equals zero. It is the maximum voltage available from a solar cell, and this occurs at zero current. The open-circuit voltage corresponds to the amount of forwarding bias on the solar cell due to the bias of the solar cell junction with the light-generated current.

$$V_{oc} = \frac{KT}{q} \ln \left(\frac{I_L}{I_o} + 1 \right) \quad (3.2)$$

Where V_{oc} is open-circuit voltage and I_L is light-generated current.

3.4.3 Fill Factor

The fill factor, more commonly known by its abbreviation "FF", is a parameter which in conjunction with V_{oc} , I_{sc} , determines the maximum power from a solar cell. The FF is defined as the ratio of the maximum power from the solar cell to the product of V_{oc} and I_{sc} . Graphically, the FF is a measure of the 'squareness' of the solar cell and is also the area of the largest rectangle which will fit in the IV curve as shown in figure 3.3.

$$FF = \frac{I_m V_m}{I_{sc} V_{oc}} \quad (3.3)$$

3.4.4 Solar Cell Efficiency

The efficiency is the most commonly used parameter to compare the performance of one solar cell to another. Efficiency is defined as the ratio of energy output from the solar cell to input energy from the sun. In addition to reflecting the performance of the solar cell itself, the efficiency depends on the spectrum and intensity of the incident sunlight and the temperature of the solar cell.

$$\eta = \frac{P_m}{P_{in}} = \frac{I_m V_m}{P_{in}} \quad \text{or} \quad \eta = \frac{I_{sc} V_{oc} FF}{P_{in}} \quad (3.4)$$

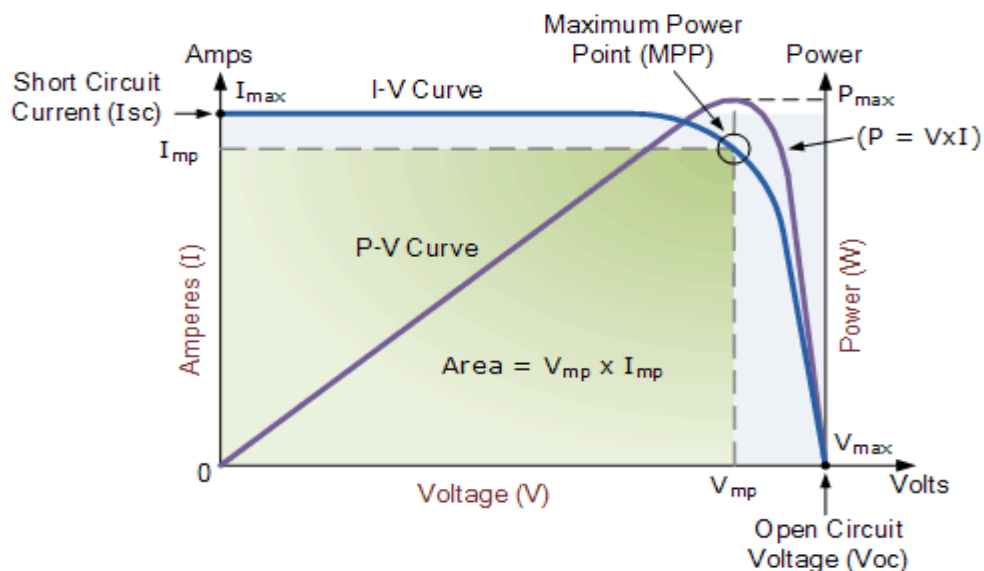


Figure:3.6 I-V curve and power curve of solar cell

CHAPTER FOUR

RESULTS AND DISCUSSION

4.1 Introduction

This chapter represents all experimental results and discussion, which related to Measurement of the Spectral Response of Silicon Solar Cell with a Set of Filters, the experimental results are represented by tables and graphs. Form the obtained results many important performance parameters such as efficiency, responsivity, and power are calculated.

4.2 the Results

The spectral response of each filter (color) obtained using the proposed monochromatic filter is graphically represented, in direct comparison to the results from the filter spectral response measurement method.

On each measuring, one filter (color band) was installed in certain location between light source and silicon solar cell and removed at the end of the test. The filters were tested sequentially, repeating the sequence several times in the measurement period, so as to minimize the influence of the changes of the light beam angle of incidence. The angle of incidence simultaneously affects both silicon solar module (as they were installed side-by-side), and the effects of location.

The electrical characteristics of the photovoltaic panels were determined under real operating conditions through an experimental work. The circuit of Figure 3.5 was used, with a power rheostat replacing the fixed-value power resistor. Furthermore, silicon solar cell is irradiated and the moment of current and voltage was registered through a portable multimeter. After

that, spectral response measurements are performed. On each filter of measurement, the short circuit current and open circuit voltage meters recorded the measuring time interval during which the silicon solar module received lamp light, and the amount of energy generated by color.

The following analysis variables are calculated with the experimental data: relative efficiency, power, responsivity. Relative efficiency is the ratio between the amount of energy generated in the solar module with the color filter and the energy produced by the module without a filter. The performance characteristics of silicon solar cell which is irradiated by tungsten lamp with different filters is achieved. Table 4.1 shows the results of the short circuit current and the open-circuit voltage while studying the current-voltage characteristics of the solar cell.

Table 4.1 measured values of the I and V

Without filter		Violet 400 [nm]		Blue 440 [nm]		Green 490 [nm]		Yellow 570 [nm]		Orange 585 [nm]		Red 620 [nm]	
V [V]	I[A]	V[V]	I[A]	V[V]	I[A]	V[V]	I[A]	V[V]	I[A]	V[V]	I[A]	V[V]	I[A]
3.21	0	2.24	0	1.83	0	0.95	0	2.61	0	1.02	0	1.12	0
3.21	1.42	2.24	0.99	1.83	0.82	0.95	0.42	2.61	1.15	1.02	0.45	1.12	0.50
2.98	1.43	2.16	0.99	1.67	0.82	0.88	0.42	2.44	1.15	0.97	0.45	1.06	0.49
2.73	1.44	2.0	1.00	1.5	0.82	0.80	0.42	2.16	1.15	0.9	0.45	0.95	0.49
2.51	1.44	1.82	1.00	1.34	0.82	0.72	0.42	1.92	1.15	0.79	0.45	0.81	0.49
2.33	1.44	1.63	1.00	1.27	0.82	0.63	0.42	1.75	1.15	0.71	0.45	0.71	0.49
2.16	1.45	1.48	1.00	1.08	0.82	0.55	0.42	1.51	1.15	0.65	0.45	0.62	0.49
1.90	1.45	1.28	1.00	0.86	0.82	0.47	0.42	1.3	1.15	0.51	0.45	0.57	0.49
0	1.45	0	1.00	0	0.82	0	0.42	0	1.15	0	0.45	0	0.49

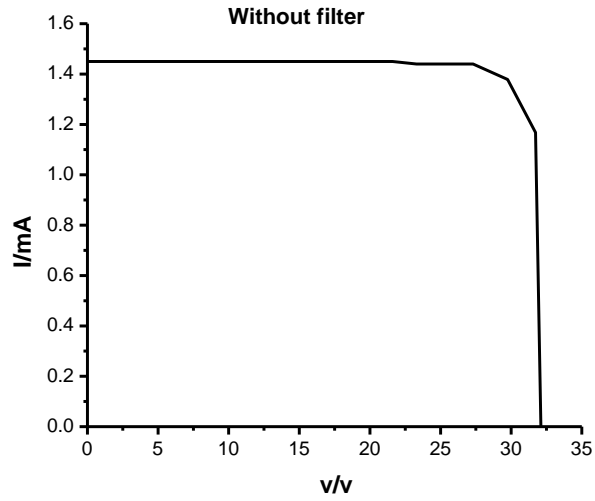


Figure 4.1: The relationship between I-V without filter

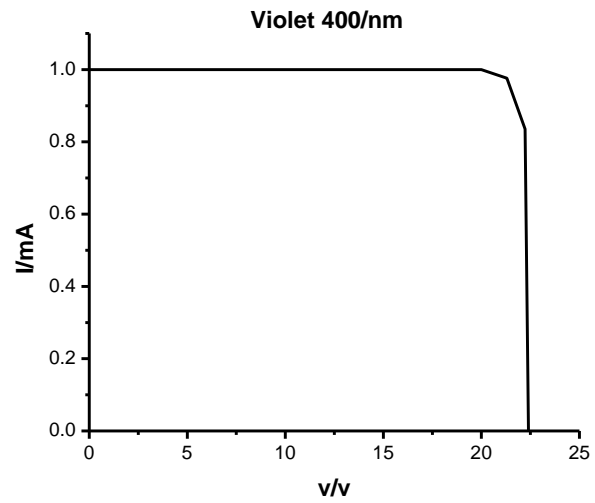


Figure 4.2: the relationship between I-V for violet 400/nm

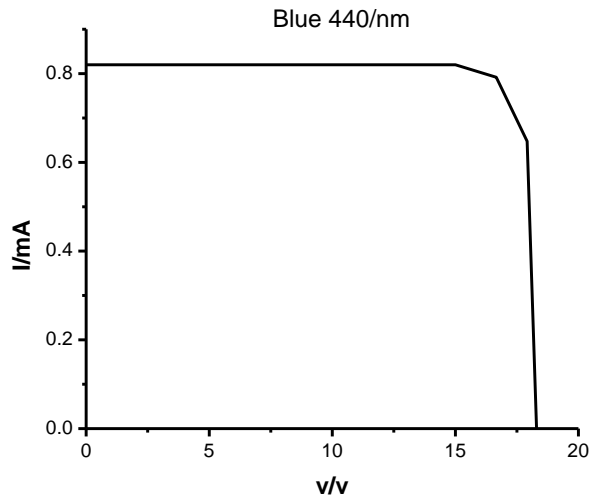


Figure 4.3: the relationship between I-V for blue 440 [nm]

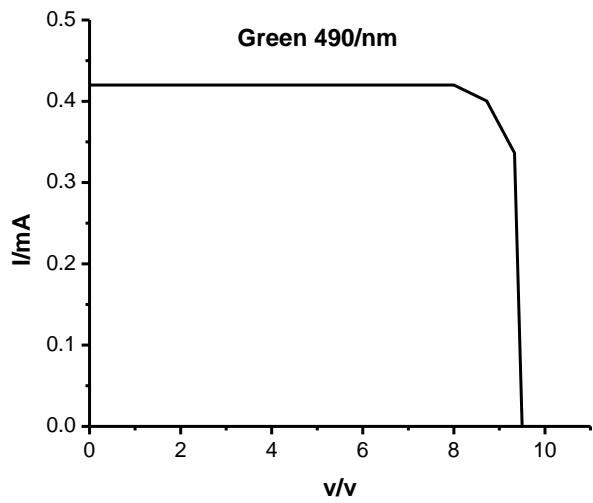


Figure 4.4: the relationship between I-V for green 490 [nm]

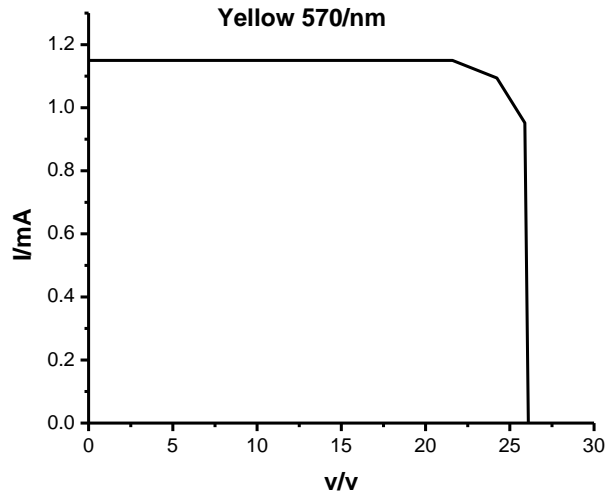


Figure 4.5: the relationship between I-V for yellow 570[nm]

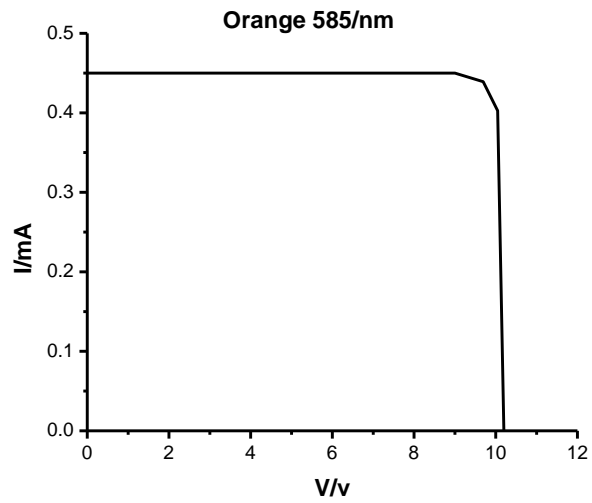


Figure 4.6: the relationship between I-V for Orange 585 [nm]

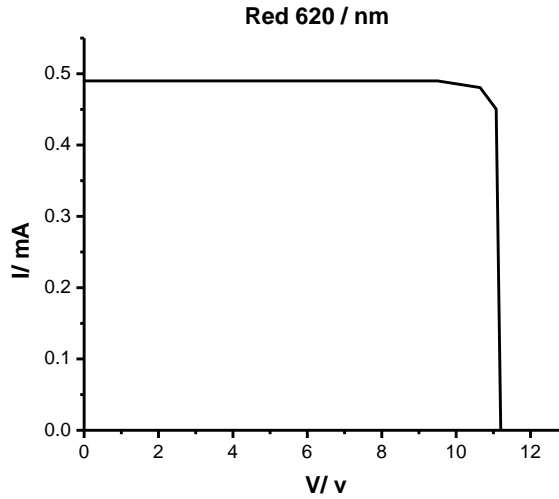


Figure 4.7: the relationship between I-V for Red 620 [nm]

Table 4.2 power, responsivity and efficiency calculations

Without filter			Violet 400[nm]			Blue 440[nm]		
P=IV[W]	Res=I/P	$\eta = P_m/P_{in}$	P=IV[W]	Res=I/P	$\eta = P_m/P_{in}$	P=IV[W]	Res=I/P	$\eta = P_m/P_{in}$
0	0	0	0	0	0	0	0	0
45.58	0.03	0.45	22.17	0.044	0.22	15	0.054	0.15
42.61	0.033	0.42	21.38	0.046	0.21	13.69	0.059	0.13
39.3	0.036	0.39	20	0.05	0.5	12.3	0.066	0.12
36.14	0.039	0.36	18.2	0.054	0.18	10.98	0.074	0.10
33.55	0.042	0.33	16.3	0.061	0.16	10	0.082	0.1
31.32	0.046	0.31	14.8	0.067	0.14	8.85	0.092	0.08
27.55	0.052	0.27	12.8	0.078	0.12	6.62	0.116	0.06
0	0	0	0	0	0	0	0	0

Table 4.3 power, responsivity and efficiency calculations

Green 490 [nm]			Yellow 570[nm]		
P=IV[mW]	Res=I/P	$\eta = P_m/P_{in}$	P=IV[mW]	Res=I/P	$\eta = P_m/P_{in}$
0	0	0	0	0	0
3.99	0.105	0.039	30.01	0.038	0.30
3.69	0.113	0.036	28.06	0.046	0.28
3.36	0.125	0.033	24.84	0.050	0.24
3.02	0.139	0.030	22.08	0.052	0.22
2.64	0.159	0.026	20.12	0.057	0.20
2.31	0.181	0.023	17.36	0.066	0.17
1.97	0.213	0.019	14.95	0.076	0.14
0	0	0	0	0	0

Table 4.4 power, responsivity and efficiency calculations

Orange 585/nm			Red 620/nm		
P=IV[W]	Res=I/P	$\eta = P_m/P_{in}$	P=IV[W]	Res=I/P	$\eta = P_m/P_{in}$
0	0	0	0	0	0
4.59	0.098	0.045	5.6	0.089	0.056
4.36	0.103	0.043	5.19	0.094	0.051
4.05	0.111	0.040	4.65	0.105	0.046
3.55	0.126	0.035	3.96	0.123	0.039
3.19	0.141	0.031	3.47	0.141	0.034
2.92	0.154	0.029	3.03	0.161	0.030
2.29	0.196	0.022	2.79	0.175	0.027
0	0	0	0	0	0

Table 4.5 Maximum Power Response versus Wavelength and efficiency

Wavelength [nm]	Maximum Power Response [A/W]	Efficiency
Violet(400)	0.044	0.22
Blue(440)	0.054	0.15
Green(490)	0.105	0.39
Yellow(570)	0.038	0.30
Orange(585)	0.098	0.045
Red(620)	0.089	0.056

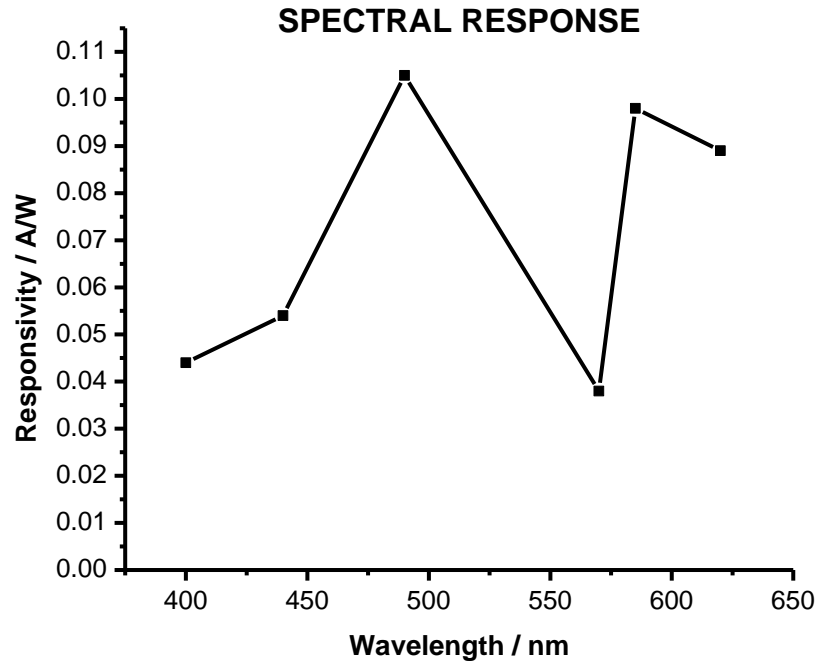


Figure: 4.8 the spectral response

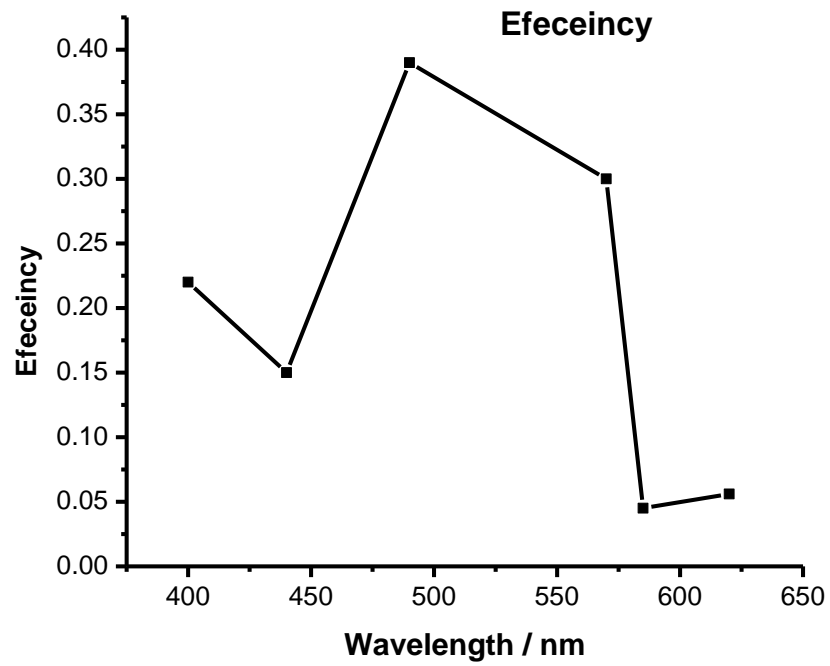


Figure: 4.9 the solar cell efficiency

4.3 Discussion

The results of sensitivity analyses of the spectral response determination to individual input parameters are shown in the following figures.

The experimental data to determine the electrical characteristics of the silicon solar module are represented Table (4.1). From this information, it can be concluded that the module have different characteristics from the nominal specifications.

Figures from 4.1 to 4.7 illustrated the current-voltage characteristic that obtained from the measured values (Table 4.1). The voltage are gradually decreased while the short circuit current increase.

From the Figure 4.8 it clear that, the highest spectral response obtained at wavelength 490 nm green color whereas the lowest spectral response at wavelength 570 nm yellow color, for the reason that of the carrier generated near the p-n junction reach the divider, therefore, photocurrent attenuation is non-existent the minimum response was at wavelength 570 nm because the short wavelengths absorbed very close to the surface and the recombination is more clarity.

Figure 4.9 shows that the highest efficiency achieved at wavelength 620 nm (red band) it was about 56%. Whilst the less efficiency was at wavelength 440 nm (blue color) it was about 15%. For the results obtained, it is clear that, the shorter wavelengths are more efficient than the longer wavelengths because the electron generation rate (electron-hole) is large because the absorption coefficient is directly proportional to the rate of generation and increase in the rate of generation increases the photocurrent which increases the open-circuit voltage and increasing the efficiency of the silicon solar cell.

From the results obtained it is clear that, the best spectral band used to irradiate silicon solar module is the green band which is appeared high efficiency. In contrast, the violet and blue bands show low response and efficiency. Yellow band shows a low response with high efficiency, and orange and red bands show high response but its efficiency was very low.

When comparing the average relative efficiency of the red, green, yellow, and blue primary filters, it can be seen that the silicon solar panel produced more energy in the green wavelength range, with a high relative efficiency of 39.0%, followed by the violet, blue, yellow, and orange ones, respectively. In this way, it can be concluded that silicon solar cell were more sensitive to radiation in the green band, which starts at about 490 nm, according to Figure 4.8. It is interesting to note that although the response to the green range was visually the greatest, the green filter was the darkest of all, which could lead to the hypothesis that this would be the filter with the lowest rate of light transmission, and consequently the lowest relative efficiency. This means that the visual appearance was not a relevant factor for its spectral response; the energy spectral distribution curve determined the response of each filter.

In particular, it is noted that the maximum power and the open circuit voltage are considerably smaller. These electrical characteristics are significantly affected by the high working temperature of the cells, which was slightly highest than the nominal test temperature. This implies lower form factors for the panels, as well as values different from nominal for the voltage and current at the maximum power. Although cell temperature is not the only major factor that influences its electrical characteristics, it plays an important role on the real energy generation capacity of silicon solar module.

Furthermore, one can note that there was a small difference in the power production between the red, green, and blue filters, ranging from 0.038 mW in the yellow one to 0.105 mW in the green ones. This shows that there is no specific and isolated range in which the production of energy is far superior or very inferior to the others. All wavelength bands contributed significantly to the generation of energy in the silicon solar cells

4.4 Conclusions

In this work the monochromatic filters method to determine silicon solar cell spectral response has been demonstrated as a feasible alternative to monochromatic filters. The way in which the electric energy generation of silicon solar cell varied according to different wavelength ranges of solar light spectrum is verified. The silicon solar cell is tested under laboratory operating conditions and is subject to environmental variations. There was a difference in the spectral response of the silicon solar cell in the red, orange, yellow, green, blue, and violet bands, with relative efficiencies. It can be concluded that silicon solar panels did not respond uniformly to tungsten lamp, being more sensitive to the green band (medium wavelengths) and less sensitive to the yellow band, although the difference between the bands was small. This analysis shows that for solar cell spectral response, use filters contributes small errors related to the source spectral profile itself. Measurement devices can cause bias errors in spectral response measurements when certain calibration procedures are employed, but such errors have no effect on performance measurements. Other error sources are likely to dominate in spectral response measurements.

The measurement devices are carefully calibrated to eliminate bias, robust against measurement noise or random uncertainties and there are no new challenges in the selection of appropriate irradiation values.

4.5 Recommendations

As a suggestion for future works, it is proposed to carry out tests of photovoltaic panels of higher power under real operating conditions in order to verify if there are significant differences in the behavior between low- and high-power modules. Other solar cell types could be investigated so that any differences in the spectral response of different photovoltaic technologies could be verified. An alternative work can be developed by replacing the color filters used (made of plastic material) with dichroic filters, which present more precise spectral distribution curves, although they have a higher cost. Finally, further investigations on the relation between the spectral response to individual wavelength ranges and the temperature increase of photovoltaic modules can be performed.

References

- After, V., Brown, S.W., Larason, T.C., Lykke, K.R., Ikonen, E. and Norma, M., 2007. Comparison of absolute spectral irradiance responsivity measurement techniques using wavelength-tunable lasers. *Applied Optics*, 46(20), pp.4228-4236.
- Aoki, D., Aoki, T., Saito, H., Magliano, S. and Takagi, K., 2012. Methods for spectral responsivity measurements of dye-sensitized solar cells. *Electrochemistry*, 80(9), pp.640-646.
- Arjun, B., 2012. *Architectural Integration of Photovoltaic and Solar Thermal Collector Systems into Buildings* (Doctoral dissertation, Master's Thesis in Sustainable Architecture. Norwegian University of Science and Technology, Faculty of Architecture and Fine Arts. Trondheim).
- Day, J., Senthilarasu, S. and Mallick, T.K., 2018. Improving spectral modification for applications in solar cells: A review. *Renewable energy*.
- Emery, K., Dunlavy, D., Field, H., and Moriarty, T., 1998. *Photovoltaic spectral responsivity measurements* (No. NREL/TP-520-25101; CONF-980735-PROC.). National Renewable Energy Lab., Golden, CO (United States).
- Hachem, M.M., 2004. BISPEC: Interactive software for the computation of unidirectional and bidirectional nonlinear earthquake spectra. In *Structures Congress 2004*. Reston, VA: ASCE.
- Historic Developments in the Evolution of Earthquake Engineering", illustrated essays by Robert Reitherman, CUREE, 1997, p10.
- Hovel, H.J., Hodgson, R.T. and Woodall, J.M., 1979. The effect of fluorescent wavelength shifting on solar cell spectral response. *Solar Energy Materials*, 2(1), pp.19-29.
- Imai, F.H. and Berns, R.S., 1999, October. Spectral estimation using trichromatic digital cameras. In *Proceedings of the International Symposium on Multispectral Imaging and*

Color Reproduction for Digital Archives (Vol. 42, pp. 1-8). Chiba University Chiba, Japan.

Kenneth W. Busch, Marianna A. Busch (1990). Multielement Detection Systems for Spectrochemical Analysis. Wiley-Interscience. ISBN 0-471-81974-3.

Li, H., Chen, C., Jin, J., Bi, W., Zhang, B., Chen, X., Xu, L., Liu, D., Dai, Q. and Song, H., 2018. Near-infrared and ultraviolet to visible photon conversion for full-spectrum response perovskite solar cells. *Nano Energy*, 50, pp.699-709.

Li, J., 2010. Application of solar energy.

Marouf, A.A., Abdullah, S.F., Abdurrahman, W.S. and Al Naimee, K., 2014. The Role of Photonic Processed Si Surface in Architecture Engineering. *Study of Civil Engineering and Architecture*, 3, pp.93-97.

Newmark, N.M., 1982. Earthquake spectra and design. *Earthquake Eng. Research Institute, Berkeley, CA.*

Paschotta, Dr. Rüdiger. "Encyclopedia of Laser Physics and Technology - responsivity, photodetectors, photodiodes, sensitivity". www.rp-photonics.com. Retrieved 2018-08-21.

Photovoltaic System Pricing Trends – Historical, Recent, and Near-Term Projections, 2014 Edition" (PDF). NREL. 22 September 2014. p. 4. Archived (PDF) from the original on 29 March 2015.

Report on the 1985 Mexico City Earthquake from "EQ Facts & Lists: Large Historical Earthquakes", USGS.

Solar Energy Perspectives: Executive Summary" (PDF). International Energy Agency. 2011. Archived from the original (PDF) on 3 December 2011.

Wang, F., Yang, M., Ji, S., Yang, L., Zhao, J., Liu, H., Sui, Y., Sun, Y., Yang, J. and Zhang, X., 2018. Boosting spectral response of multi-crystalline Si solar cells with Mn²⁺ doped CsPbCl₃ quantum dots down converter. *Journal of Power Sources*, 395, pp.85-91.